JOURNAL OF EXPERIMENTAL AND THEORETICAL PHYSICS, 2024, Vol. 166, No. 1(7), pp. 69–82

PROGRESS, PROBLEMS AND PROSPECTS OF ROOM-TEMPERATURE SUPERCONDUCTIVITY

© 2024 I. A. Troyan[a], D. V. Semenok[b], A. V. Sadakov[c], I. S. Lyubutin[a], V. M. Pudalov[c,d,*]

[a] *Shubnikov Institute of Crystallography, Kurchatov Complex of Crystallography and Photonics, National Research Center "Kurchatov Institute", Moscow 119333, Russia*

[b] *Center for High Pressure Science and Technology Advanced Research (HPSTAR), Beijing 100094, China*

[c] *Ginzburg Research Center for High-Temperature Superconductivity and Quantum Materials, Lebedev Physical Institute, Russian Academy of Sciences, Moscow 119333, Russia*

[d] *National Research University Higher School of Economics, Moscow 101000, Russia*

**e-mail: pudalovvm@lebedev.ru*

Received May 08, 2024

Revised May 14, 2024

Accepted May 15, 2024

Abstract. The discovery of superconductivity at megabar (MB) pressures in hydrogen sulfide H_3S, followed by metal polyhydrides, starting with binary ones, LaH_{10} etc., and ending with ternary ones, including $(La,Y)H_{10}$, has revolutionized the field of condensed matter physics. These discoveries strengthen the hope for solving the century-old problem of creating materials with room-temperature superconductivity. In experiments performed at MB pressures over the past 5 years, besides the synthesis of hydrides, their physical properties were studied using optical, X-ray and Mössbauer spectroscopy methods, as well as galvanomagnetic measurements. We present the main results of galvanomagnetic measurements, including measurements in strong static (up to 21 T) and pulsed (up to 70 T) magnetic fields. Measurements of resistance drop to vanishingly small values at temperatures below the critical T_c value, decrease of critical temperature T_c with increasing magnetic field, as well as diamagnetic screening indicate the superconducting state of polyhydrides. The results of isotope effect measurements, together with the effect of magnetic impurities on T_c, indicate the electron-phonon mechanism of electron pairing. However, interelectron correlations in polyhydrides are by no means small in both superconducting and normal states. Possibly, this is the origin of unusual properties of polyhydrides that have not yet received a satisfactory temperature explanation, such as the linear temperature dependence of the second critical field $H_{c2}(T)$, linear resistance dependence $\rho(T)$, as well as linear magnetoresistance, very similar to that discovered by P. L. Kapitsa in 1929.

Article for the special issue of JETP dedicated to the 130th anniversary of P. L. Kapitsa

DOI: 10.31857/S004445102407e083

The authors dedicate this article to the memory of P. L. Kapitsa, whose experiments in the 1920-30s stimulated research in strong magnetic fields and at low temperatures in Russia. One of the authors (V. M. P.) is grateful to P. L. Kapitsa for the opportunity to work for several years in the unforgettable creative atmosphere of the Institute for Physical Problems.

1. HISTORICAL INTRODUCTION. BRIEF CHRONOLOGY OF DISCOVERIES

The history of superconductivity (SC) began in 1908 when Kamerlingh Onnes liquefied helium and subsequently (1911) discovered the disappearance of resistance in a mercury wire immersed in liquid helium.

In the following fifty years, up until the 1960s, many superconducting metals and intermetallic superconducting compounds were discovered. The

most widely used intermetallics – a class NbTi ($T_c = 9.8$ K) and Nb_3Sn ($T_c = 18$ K) are representatives of type-II superconductors, discovered by L. V. Shubnikov in the 1930s. Finally, in 1986 K. Mueller and G. Bednorz discovered superconductivity in ceramic compounds based on copper oxide. In this class of compounds, the record-high $T_c = 138$ K belongs to the compound HgBaCaCuO(F), while $YBa_2Cu_3O_{7-x}$ and $GdBa_2Cu_3O_{7-x}$, are used for widely practical applications, having a critical temperature ~ 93 K.

The most famous and widespread mechanism of Cooper pairing of electrons through electron-phonon interaction obviously leads to the dependence of T_c on the mass of crystal lattice atoms. Since hydrogen is the lightest element, researchers' attention has long been focused on it. The possibility of transition to metal in highly compressed hydrogen was first suggested in 1935 [1], and in 1968, Ashcroft [2], and then in 1989, Barbie et al. [3] predicted that the critical temperature of transition of the metallic phase of hydrogen to the SC state could reach about 200–400 K. Atomic metallic hydrogen in solid form has not yet been obtained under static conditions, as this requires gigantic pressures of about 400–500 GPa.

In 2004, Ashcroft suggested that hydrogen-rich compounds could have high critical temperatures [4], and the pressures required for this should be significantly lower than the pressures necessary to convert hydrogen into a metallic superconducting state. In 2006, work [5] predicted high-temperature superconductivity in silane SiH_4. This prediction was only partially confirmed: silane indeed demonstrated a superconducting state at a pressure of 100 GPa, however, its critical temperature was only 17 K [6]. Nevertheless, Ashcroft's proposal stimulated intensive experimental searches for superconducting hydrides, which culminated in 2015 with the discovery of superconductivity in H_3S by M. E. Eremets' group [7, 8]. The increase in critical temperature ($T_c = 205$ K) by more than 60 K compared to that achieved in copper oxides demonstrated the potential capabilities of superconducting hydrides and gave a powerful impulse to their further research.

To date, numerous metal hydrides have been discovered that become superconducting at high pressure with critical temperatures up to 250–260 K, as a result, polyhydride superconductivity has formed as a separate and most interesting area of research.

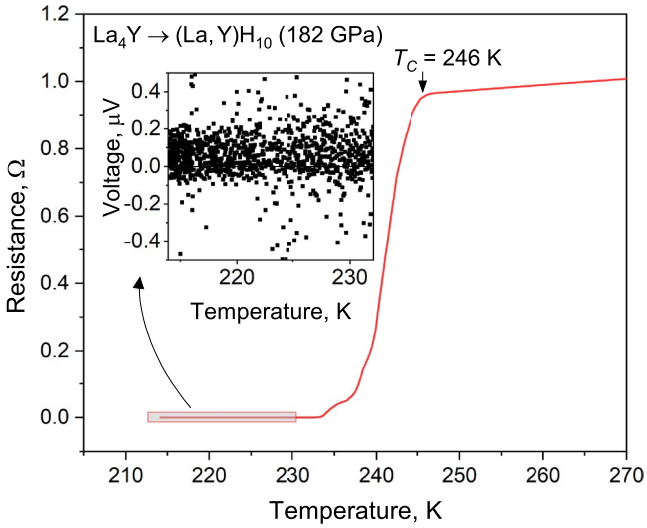

Fig. 1. Temperature dependence of resistance during superconducting transition in $(La,Y)H_{10}$ at pressure of 182 GPa. The inset shows, in enlarged scale, the voltage drop at potential contacts in the superconducting state at measuring current of 1 mA

2. KEY RESULTS OF POLYHYDRIDE RESEARCH

2.1. Disappearance of electrical resistance

In hydrides of lanthanum, yttrium, thorium, etc., a sharp drop in electrical resistance is observed when temperature decreases below critical T_c, while the value of T_c depends on pressure. When the 4-probe method is used, resistance measurement at $T < T_c$ gives a value at noise level, less than 0.1 mΩ [9, 10] (Fig. 1).

The application of an external magnetic field reduces the temperature of the superconducting transition and also broadens the transition itself. Due to the extremely high values of the upper critical magnetic field (which destroys superconductivity), the broadening becomes noticeable only starting from high fields. Fig. 2 demonstrates the influence of the magnetic field on the superconducting transition in $(La,Y)H_{10}$ [9].

2.2. Isotope Effect

One of the most important results indicating the electron-phonon mechanism of superconductivity in hydrides is the isotope effect. This effect manifests in the decrease of the superconducting transition temperature when hydrogen is replaced with heavier

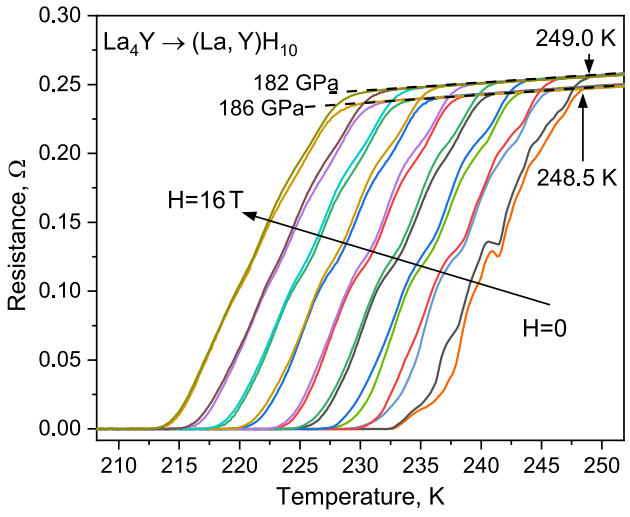

Fig. 2. Change in temperature dependence of resistance in external magnetic field below critical value in (La, Y)H_{10}. Results are shown for two pressure values, 182 and 186 GPa. External magnetic field varies (along the arrow, right to left) from 0 to 16 T in 2 T steps. Numbers with vertical arrows at the top of curves mark critical temperature values at $H = 0$ for 2 pressure values. Adapted from work [9]

deuterium atoms in the compound structure. This effect was observed for H_3S [7], LaH_{10} [11], YH_6 [12], YH_9 [13], CeH_{9-10} [14] and several other compounds In all cases, the isotopic coefficient $\alpha = -\ln(T_c)/\ln(M)$, where M is atomic mass, falls within the interval $-0.3 - 0.6$, in reasonable agreement with BCS theory prediction.

A certain complexity in the analysis is introduced by the fact that the ionic radius and bond energy of deuterium and hydrogen differ, and the stability limits on the pressure scale and areas of structure distortion for hydrides and deuterides differ to an even greater extent. For this reason, comparing T_c values for hydrides and deuterides at the same pressure is sometimes incorrect, as they may have different crystal structures. Another factor complicating the comparison is the significantly lesser influence of anharmonicity on superconductivity in deuterides.

In general, deuterides exhibit the same properties as hydrides, namely, the superconducting transition shifts depending on the applied magnetic field; the upper critical field $H_{c2}(0)$, being proportional to T_c, in deuterides is typically significantly lower than in hydrides, and finally, there exists a critical current whose value also depends on the magnetic field. With pressure reduction, the critical temperature of the SC transition in deuterides noticeably decreases, and then the compound decomposes forming lower deuterides and D_2 [10].

As an example, Fig. 3 shows that the critical temperature decreases when hydrogen is replaced with a heavier element, and this relationship holds true across a wide pressure range from 175 to 250 GPa.

2.3. Effect of magnetic and non-magnetic impurities on critical temperature

2.3.1. Magnetic impurities

The introduction of impurities into a superconductor is an important tool for studying symmetry and

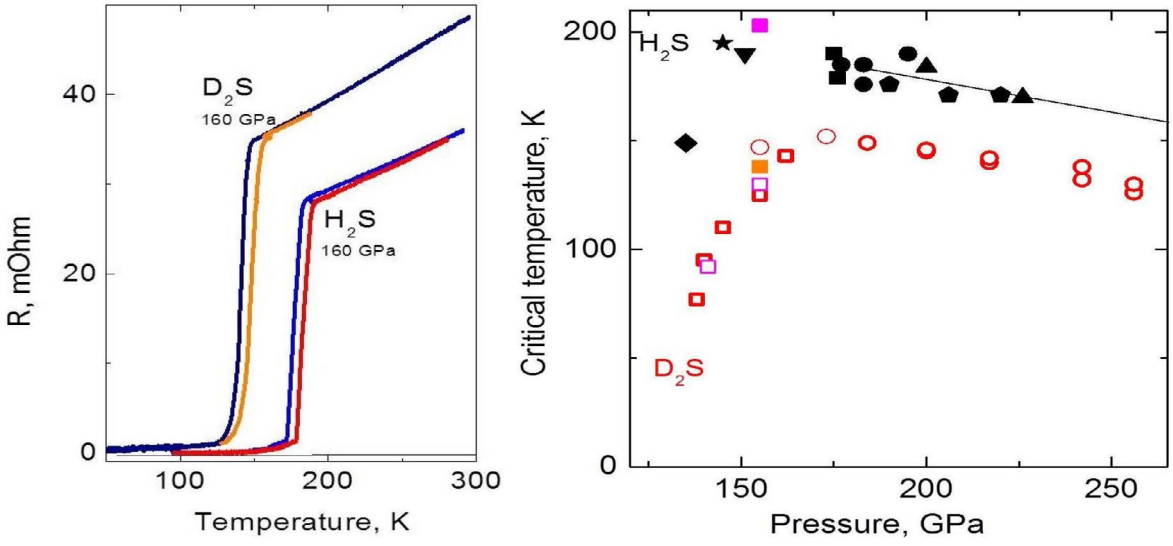

Fig. 3. Superconducting transition curves by resistance (left panel) and critical temperature dependence on pressure (right panel) for H_2S and D_2S. Adapted from work [7]

pairing mechanism. According to Anderson's theorem [16, 15], non-magnetic impurities do not affect the isotropic singlet *s*-wave order parameter in conventional BCS-type superconductors [17], while scattering on paramagnetic centers effectively destroys *s*-wave type pairing [16, 18].

In work [19], a series of ternary polyhydrides with composition (La, Nd)H_{10}, containing 8–20 at. % Nd was synthesized. The Nd^{3+} ions have an outer electron shell $4f^3$ and magnetic moment $3.62\mu_B$/atom. Since Nd atoms are randomly distributed in the lattice, they can be considered as paramagnetic impurities. The main idea of this experiment was that Nd should effectively suppress superconductivity in LaH_{10},while its structure $Fm\bar{3}m$ remains practically unchanged due to the great similarity of physical properties between La and Nd atoms.

For small concentrations of magnetic impurities, $x \ll 1$, the Abrikosov–Gorkov theory predicts a linear dependence of T_c on concentration x [16, 18]:

$$T_c(0) - T_c(x) = \frac{\pi\hbar}{4k_B\tau}x, \qquad (1)$$

where τ is the collision time for scattering on random impurity potential.

In the case of (La,Nd)H_{10}, $\tau \approx 5.4 \cdot 10^{-15}$s [19]. According to (1), each percent of Nd impurity content should lower T_c in LaH_{10} by $\Delta T_c \approx 10$ K, or, in relative units, $\Delta T_c(1\%\mathrm{N}d) / T_c(\mathrm{L}aH_{10}) = 0.044$. Comparing this with the experimental data shown in Fig. 4, we see good agreement between theoretical predictions and experimental data. It has been established that superconductivity completely disappears at approximately 20% Nd impurity content (see [19], Supplementary material).

For comparison with conventional low-temperature BCS superconductors, we note that in work [20], the suppression of metallic La superconductivity by magnetic impurities Eu and Gd was also studied. Agreement with theory [18] was found when accounting for corrections due to reduced scattering cross-section on Eu impurities compared to Gd impurities (due to smaller exchange overlap integral of 4*f*–5*d*-states).

2.3.2. Non-magnetic impurities

Regarding non-magnetic impurities, it is known that the introduction of a small concentration of carbon in La does not affect the critical temperature of superconductivity in C:LaH_{10}, $T_c \approx 245$ K (see note in work [19]). Numerous experiments with high-pressure cell assembly in air with metals Y, La Y, La Nd, with inevitable presence of oxide film on metal surfaces, qualitatively confirm the absence of influence of non-magnetic oxygen impurities on the critical temperature of hydrides.

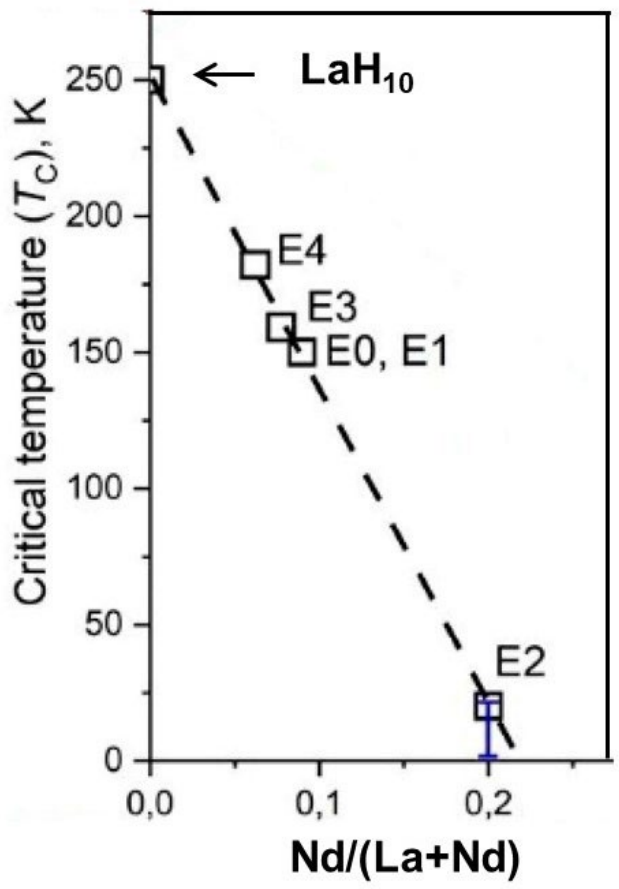

Fig. 4. Dependence of critical temperature (La,Nd)H_{10} on relative concentration of Nd impurities. The arrow marks the value T_c for stoichiometric LaH_{10}. Adapted from work [19]

Another example is a recent work on introducing sulfur into yttrium polyhydrides [21], where the authors observed steps in the temperature dependence of electrical resistance corresponding to $T_c = 235$ K and about 210–215 K. These values agree with previously obtained results for YH_6 and YH_9, indicating no influence of non-magnetic sulfur on the critical temperature of yttrium hydrides. Indirect confirmation of the absence of non-magnetic impurities' influence is also shown by almost identical values of

T_c = (176–203) K in compounds $R\bar{3}m$-(La, Y)H_{20} and $Pm\bar{3}m$-(La, Y)H_{12} (see Table 2 in work [19]), differing, in this context, by concentration of non-magnetic atoms.

The most important effect of impurities on polyhydrides is the change in their dynamic and thermodynamic stability regions. A striking example is the synthesis of lanthanum-cerium hydrides (La, Ce)H_{9-10}, which currently demonstrate the highest T_c at the lowest pressure: $T_c > 200$ K at 100 GPa [22, 23].

Among pathological reports (about materials now commonly referred to as "unidentified superconducting objects", USO) we note in a recent announcement about the "miraculous" effect of carbon doping on superconductivity H_3S [24]. Subsequent experimental works did not confirm this result [25, 26], analysis of the experimental data itself revealed their falsification [27], and the corresponding report was retracted from the journal.

The compound LuH_xN_y should be discussed separately. The report that this compound, when doped with non-magnetic nitrogen atoms, transitions to a superconducting state with $T_c = 294$ K at a pressure of only 10 kBar [28] also proved to be doubtful. It was refuted by subsequent works and the corresponding article was retracted [29].

However, the theoretically predicted positive result of doping on the value of T_c is interesting. According to band structure calculations [30], it is achieved when nitrogen atoms are incorporated not in random positions but in regular positions of the crystal lattice, replacing 1/4 hydrogen atoms. As a result of such special substitution, the Fermi level in $LuH_{2.75}N_{0.25}$ decreases by ≈ 1.8 eV compared to LuH_3. Simultaneously, the density of states at the Fermi level increases almost twofold. However, it remains unclear whether such substitution is feasible in practice.

2.4. Meissner Effect and Diamagnetic Screening

Measurements of electrical resistance drop (Figs. 1, 5) are necessary but not sufficient to prove the existence of superconductivity. In addition, direct observation of magnetic field expulsion from the sample volume (Meissner effect) in an external magnetic field is required. However, measurements of the Meissner effect using SQUID magnetometer or inductive method at pressures above 130 GPa are difficult, as the signal from the sample in the diamond anvil cell is typically orders of magnitude smaller than the signal from the materials used to make the cell and gasket. Nevertheless, experiments to observe diamagnetic screening in hydrides were performed using SQUID magnetometry [8, 31–35], AC magnetic susceptibility measurements [32, 33] and Mössbauer spectroscopy [36].

In all experiments so far, it has only been possible to observe the absence of magnetic field in the volume of a sample pre-cooled in zero field (ZFC mode). Obviously, this is a manifestation of the "diamagnetic screening" effect. For the reason noted above, it has not yet been possible to observe true magnetic field expulsion from the sample when cooling it in the presence of a field (FC) [37]. It should be noted that while the superconducting transition is pronounced in ZFC measurements, its signs are barely distinguishable or almost undetectable in measurements with cooling in a magnetic field (FC) [31].

In addition to technical problems associated with magnetic measurements in diamond anvil cells, there are also peculiarities in the displacement of weak magnetic flux in type-II superconductors related to strong vortex pinning [38]. Strong pinning prevents vortices from moving into and out of the sample interior below $H_{c1}(T)$. As shown in works [39, 40], in a type-II superconductor (which SC-hydrides certainly are) Abrikosov vortices and magnetic field in the center of the sample are absent until the external field is less than the full penetration field H_p. The corresponding analysis of this effect for specific measurements with H_3S was conducted in work [10]. It was shown that in the field range $H_{c1} < H < H_p$ the distribution of Abrikosov vortices in the sample should be inhomogeneous, as in all type-II superconductors, and the magnetic flux density decreases from the sample edges to the center. Therefore, formulas for uniform field are not applicable to such experiments, as they use an overestimated value of H_{c1}. The values of H_{c1} and critical current j_c obtained for H_3S as a result of analysis [10] well correspond to similar parameters for other type-II superconductors.

In work [36], a different method was used for detecting diamagnetic properties of superconducting hydrogen sulfide at high pressures, namely, Mössbauer spectroscopy [41, 42]. The magnetic field detector was a thin tin foil enriched with the Mössbauer isotope Sn-119. The magnetic moments

of Sn-119 nuclei are an order of magnitude larger than those of the traditionally used Mössbauer iron isotope Fe-57, therefore Sn-119 nuclei are more sensitive to magnetic environment than Fe-57 nuclei. During nuclear gamma resonance, Mössbauer spectra are recorded for transitions between nuclear levels of ground and excited states of Sn-119 nuclei with spins 1/2 and 3/2, respectively.

Synchrotron experiments were performed in Nuclear Resonance Forward Scattering (NRS or NFS) mode for two magnetic field directions – parallel and perpendicular to the sample plane. In this mode, synchrotron radiation consists of picosecond pulses with time intervals between them reaching 800 ns or more. During this period, the time decay of radiation from Mössbauer isotope nuclei is recorded after pulse resonant excitation. The shape of the spectra depends on the magnetic state of the sample. In the absence of a magnetic field on the sample, the nuclear scattering signal has an exponentially decaying form. In the presence of a magnetic field, so-called quantum beats appear, caused by radiation interference during transitions between ground and excited states of nuclei Sn-119, split by the magnetic field. In nuclear resonance scattering spectra, this manifests as oscillations in signal amplitude.

In these measurements [36], the Mössbauer sensor showed the magnitude of the magnetic field that penetrated the sample at a given temperature. It was established that in the temperature range 4.7–90 K the superconductor H_3S completely shields the Mössbauer sensor from the magnetic field. Above this temperature, the external magnetic field partially penetrates the sample, however, complete field penetration occurs only above 145 K. The obtained data confirm the diamagnetic shielding effect in H_3S magnetic field of 0.7 up to temperatures 90–100 K. Partial magnetic field shielding persists up to approximately 145 K. This confirms that sulfur hydride H_3S, compressed to 150 GPa, is a type-II superconductor with very high critical parameters.

When analyzing the results of diamagnetic screening studies in samples LaH_{10} and H_3S using a SQUID magnetometer, it should be considered that the hydride samples are likely porous and consist of microscopic grains (about 0.05–0.5 μm). In this case, the demagnetization factor N should be calculated for random packing of spherical particles and ranges from 0.33 to 0.5 [43, 44]. Magnetic field penetrates the sample between individual grains, therefore no change in sample magnetization is observed at temperatures around T_c during field cooling (FC). Thus, the found penetration field values of $H_p(0) = 96$ mT for H_3S and 41 mT for LaH_{10} represent the lower bound of $H_{c1}(0)$, while a more realistic estimate gives $H_{c1}(0) \sim H_p(0) / (1 - N) = (1.5 - 2) \cdot H_p(0)$.

3. UNUSUAL TRANSPORT PROPERTIES OF HYDRIDES IN S AND N STATES

3.1 Upper critical field

In the Ginzburg–Landau theory [45], the upper critical field equals

$$H_{c2}(T = 0) = \frac{\phi_0}{2\pi\xi_0^2}, \qquad (2)$$

where ϕ_0 is the magnetic flux quantum and ξ_0 — the coherence length.

Due to extremely high values of the upper critical field $H_{c2}(T = 0)$, the influence of magnetic field on the superconducting transition in hydrides can usually be traced only in the high-temperature region, near T_c. To study the dependence of $H_{c2}(T)$ in a wider range of normalized values T / T_c compound SnH_4 with relatively low value of $T_c \approx 72$ K was investigated in work [46] (see Figs. 5 and 6). One of the possible reasons for such a low value of T_c is the low density of electronic states at the Fermi level [46].

The temperature dependence of H_{c2}, measured in a constant field of a superconducting magnet, is shown in Fig. 6 *a*. At $T \to 0$ this dependence extrapolates to $H_{c2}(T = 0) \approx 16$ T; such a low value of $H_{c2}(0)$ allowed measuring this dependence in the entire field range, from 0 to $H_{c2}(T = 0)$. The temperature transition broadening, shown in Fig. 6 *b*, illustrates the above statement that $\Delta T_c / T_c$ changes weakly in low fields but then sharply increases as the field increases.

The most interesting and unusual result is the functional dependence $H_{c2}(T)$: it is practically linear across the entire temperature range up to T_c. When measured in a pulsed field up to 68 T, a linear dependence $H_{c2}(T) \propto (T_c - T)$ was also discovered [19]. For superconductors described by the Bardeen–Cooper–Schrieffer (BCS) theory, the commonly accepted model for the dependence

$H_{c2}(T)$ is the Werthamer–Helfand–Hohenberg (WHH) model, which predicts flattening of the $H_{c2}(T)$ dependence at low temperatures [47].

The linear dependence $H_{c2}(T)$ is not unique to SnH_4, it is observed in many other polyhydrides, for example, in YH_4, LaH_x and others. Similar linear or quasi-linear dependence $H_{c2}(T)$ was also observed in iron pnictides [48–50], and in some cases it could be explained by the presence of multiple superconducting gaps in the spectrum [48–51]. An example of attempting to describe the measured dependence $H_{c2}(T)$ within the framework of a two-component so-called alpha-model of the superconducting condensate is shown in Fig. 7 (see [46], Supplementary Information).

Indeed, for most polyhydrides, due to the large number of electrons per unit cell, many bands are filled and the Fermi surface (FS) is multi-band. Furthermore, for several polyhydrides (LaH_{10}, YH_{10}, YH_9) the existence of a two-component SC condensate has been theoretically predicted [52, 53, 54]. However, such an explanation is not universal, since superconductivity, for example, in CaH_6, according to theoretical results [55], is single-gap.

An alternative explanation for the linear dependence $H_{c2}(T)$ could be mesoscopic inhomogeneity of samples, which contain regions with slightly different composition and different values of T_c and H_{c2} [19, 56, 57] in their volume. Indeed, despite the sharp drop in resistance during the superconducting transition and the conducted X-ray data indicating macroscopic homogeneity of SC-hydrides, the existence of inhomogeneities at mesoscopic scales cannot be excluded. Theoretical models do not fully explain the linear dependence $H_{c2}(T)$. Moreover, paper [56] predicts some straightening of the standard BCS dependence due to the appearance of a section with positive curvature in the dependence $T_c(H)$. The model [57] predicts an increase in H_{c2} at $T \to 0$. As long as the superconducting regions in the sample volume are connected via Josephson tunnel coupling, superconductivity will manifest itself in the sample volume.

The linear dependence $H_{c2}(T)$ was previously observed in InO films, and to explain it, paper [58] suggested that the SC state is a vortex glass state, where thermal fluctuations lead to such dependence. For SC-hydrides, scaling analysis of critical current in ThH_{10} [59] revealed the dependence $j_c \propto (1 - T / T_g)^{1.6}$, where T_g was interpreted as the transition temperature to the vortex glass state. The dependence with such power exponent does not contradict the Ginzburg-Landau theory result $j_c \propto \rho_s / \xi_{GL} \propto (1 - T / T_c)^{3/2}$, however, such interpretation and its applicability to polyhydride results require more detailed study.

Note also that for a typical hydride CeH_{9-10} the Fermi temperature $T_F \approx 6.5 \cdot 10^4$ K. Therefore, the ratio $T_c / T_F \sim 1.5 \cdot 10^{-3}$ is not small, unlike simple superconducting metals (e.g., Sn, In, etc.), where this ratio $\sim 10^{-5}$. For higher-temperature hydrides, the ratio T_c / T_F is rather close to iron-based pnictide superconductors and cuprate superconductors. Similarly, the ratio $2\Delta(0) / T_c \approx 4$ [60] is not small. For these reasons, SC-hydrides should be considered as moderately strong coupling superconductors.

3.2. Linear temperature dependence of resistance

In the normal state, the transport properties of SC hydrides are still not fully understood. In many hydrides over a wide temperature range, $T > T_c$ in the absence of a magnetic field, a linear temperature dependence of resistance is observed: this dependence is visible in Fig. 5 in the range $T = 120$–320 K.

A similar temperature dependence $R(T)$ was observed in LaH_{10} [19, 61], in CeH_{9-10} [62] and in several other hydrides. In all cases, it is linear; for example, for CeH_{9-10} — in the range ~ 110–300 K [62]. Also, in all these cases, the linear resistance dependence cannot be approximated by the Bloch-Grüneisen dependence [63] for electron-phonon scattering. Indeed, attempting such approximation for SnH_4 leads to an unrealistically low Debye temperature of approximately 100 K [46], which contradicts the phonon spectra of hydrides with strong peaks of hydrogen atom vibrations at high frequencies.

Talantsev [60] successfully approximated $\rho(T)$ for $(Ln,Nd)H_{10}$ with the dependence T^5 and obtained a plausible estimate of $\theta_D = 1150$ K. However, the experimental data $\rho(T)$ for this compound barely deviated from the linear dependence, making the approximation result unreliable. Note that in many other cases (example shown in Fig. 5), the deviation of the measured $R(T)$ from a linear function is even smaller. For example, for SnH_4 when

approximating experimental data $\rho(T)$ with function $R = R_0 + AT^n$ with fitting parameter n in work [46] the value $n = 0.9$, was obtained, which contradicts the expected value $n = 5$ (see Fig. 22 in work [46], Supplemental Materials).

Moreover, if the dependence $R(T)$ in zero magnetic field arose due to phonon scattering and was described by the Bloch-Grüneisen formula, then the application of a magnetic field would have no effect on it. Indeed, the magnetic field changes neither the phonon spectrum nor the matrix element of electron-phonon scattering. However, it has been experimentally established [64] that applying a field 20 T to (La, Ce) H_{10} at 148 GPa changes the situation and "straightens" the dependence $R(T)$ to linear, thus excluding the possibility of its approximation $\propto T^5$. Therefore, this result (straightening of $R(T, H \neq 0)$) indicates a non-phonon mechanism of the linear dependence $R(T)$.

Not many physical mechanisms are known that lead to a linear temperature dependence of metal resistance. To evaluate their applicability, note that the hydrides in the normal state have a Fermi energy $T_F \approx (3-10)\cdot 10^4$ K, carrier concentration $n = (20-60)\cdot 10^{21}$ cm^{-3} and are good metals, $E_F\tau / \hbar \gg 1$. The dimensionless electron-electron interaction parameter $r_s = E_{ee} / E_F$ in the normal state for hydrides is not small; for example, for CeH_9 [62] it is $r_s \approx 2.5$. For a strongly correlated normal metal, positive temperature dependence $d\rho / dT > 0$, in principle, can arise due to electron-electron interaction assisted scattering on impurities. For the estimated concentration above, the Fermi-liquid constant $F_0^a \approx -0.2$, therefore Fermi-liquid effects should not be small [65]. However, only for the two-dimensional case do they lead to a linear dependence $\rho(T) \propto T$ [66] and only in the ballistic interaction regime $k_B T\tau / \hbar \gg 1$, while for the three-dimensional case – to the dependence $\propto T^{1/2}$ [65], which does not correspond to the observed linear one.

For completeness, note that the linear dependence $\rho(T)$ exists in the normal state not only in hydrides but also in other HTS materials – iron pnictides ($FeSe_{1-y}S_y$), nickelates $La_3Ni_2O_7$ [67] and cuprates ($La_{2-x}Sr_xCuO_4$) [68]. In all cases, it has not yet found a satisfactory explanation.

3.3 Linear magnetoresistance

In many polyhydrides in the normal state in weak magnetic fields, the electrical resistance increases quadratically with increasing field (see Fig. 8), which is typical for a multiband metal (one could even say that such magnetoresistance indicates a multiband FS). However, with further increase in the field, this dependence changes and the resistance begins to increase linearly and continues to grow this way up to the maximum field values available in the laboratory.

Linear dependence of magnetoresistance on field was discovered by P.L. Kapitsa in 1929 [69] for polycrystalline samples. Dreizin and Dykhne [70] explained linear magnetoresistance by accounting for scattering at crystallite boundaries in strong magnetic fields $\omega_c\tau \gg 1$. Additionally, Kapitsa's law in polycrystals arises from averaging over angles of the polar diagram of magnetoresistance for metals that have open sections of the Fermi surface (for example, Cu, Ag, Au, In, Pb). In hydrides, the presence of open sections of the Fermi surface indeed follows from band structure calculations for several compounds, for example, LaH_{10} and YH_6 [71, 72], but experimentally open sections of the Fermi surface have not yet been detected.

Besides hydrides, linear dependence $R(H)$ is observed in quasi-two-dimensional "bad metals" — $SrZnSb_2$ [73], in semimetals — $Ni_3In_2S_2$ [74], and also in ferromagnetic MnBi [75]. In compounds with charge density wave (CDW) and incomplete Fermi surface nesting, linear magnetoresistance is also observed at temperatures below the CDW onset temperature: in quasi-one-dimensional compounds (for example, $NbSe_3$ [76]), in quasi-two-dimensional transition metal dichalcogenides (for example, 2H-$NbSe_2$ and 2H-$TaSe_2$ [77]) and in rare-earth tritellurides (for example, $TbTe_3$ and $HoTe_3$ [78]). Such dependence is associated with charge carrier scattering on CDW order parameter fluctuations [78].

Polyhydrides, however, in their normal state are good metals; they do not possess one-dimensional or two-dimensional spectrum character, nor ferromagnetism. The temperature dependence of polyhydride resistance shows no signs of transition to CDW state.

Finally, linear magnetoresistance is observed in materials with Dirac spectrum, for example, in graphene, gapless semiconductors, or layered semimetals with very low carrier concentration [79, 80], however, such spectrum and such low

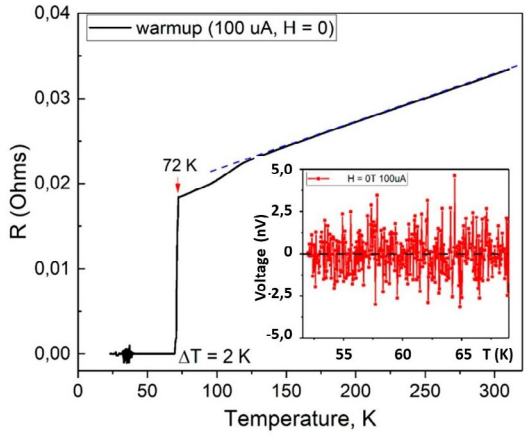

Fig. 5. Superconducting transition curve by resistance for tin hydride at 180 GPa pressure. Inset: voltage drop between potential contacts to the sample in the superconducting state at measuring current of 100 μA. Adapted from work [46]

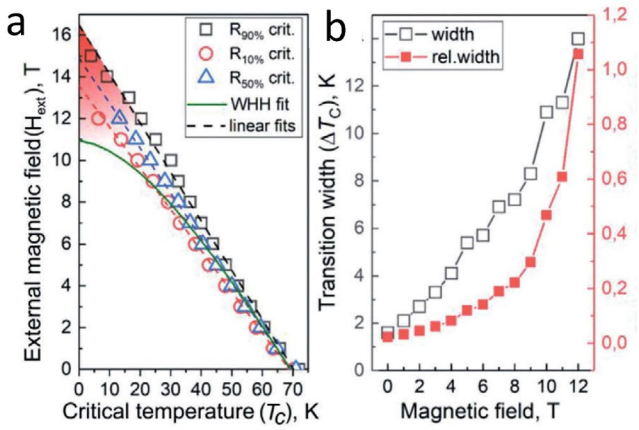

Fig. 6. *a* — Temperature dependence of the upper critical field for SnH_4using three different criteria for determining the value of H_{c2}; the solid line shows the approximation using the WHH [47]. *b* — Dependence of the transition width ΔT_c and relative transition broadening ΔT_c / T_c on the magnetic field. Adapted from work [46]

carrier concentration are also not characteristic of polyhydrides.

Recently, it was discovered that many polyhydrides, for example, La_4H_{23} [81], CeH_{10} [82], ThH_9 and (La, Ce)H_{10} exhibit negative magnetoresistance above the superconducting transition in strong magnetic fields. It can be assumed that such behavior is related to the presence of a pseudogap state in hydrides, just as observed in cuprate superconductors.

4. CONCLUSION

Superconducting polyhydrides with critical temperatures near room temperature values, as very "young" materials, attract close attention of researchers. The most evident and allowing simple interpretation are the results of transport and magnetic properties measurements. Numerous galvanomagnetic measurements have documented and reproduced results of measuring resistance drop at temperatures below the critical value T_c, indicating a superconducting transition. In magnetic measurements, static diamagnetic screening was also repeatedly observed when applying external field to a sample cooled in zero field (ZFC). These experiments were carried out using magnetic moment measurements and magnetic susceptibility by SQUID magnetometer and using the Mössbauer effect with synchrotron gamma-ray radiation. Due to technical difficulties in measuring small signals, unfortunately, it has not yet been possible to reliably register the expulsion of magnetic field from the sample volume when cooling it in a magnetic field (FC), i.e., the true Meissner effect. Such measurements would be very important to prove the truly superconducting state. The observation of isotope effect in superconducting hydrides is convincing evidence of electron-phonon pairing mechanism. Experiments on the influence of magnetic impurity scattering on critical temperature are in agreement with Abrikosov–Gorkov theory and prove the singlet nature of superconducting pairing.

As a result of the listed experimental findings, independently reproduced in several laboratories, it is currently accepted that hydrides belong to conventional superconductors with singlet pairing and moderately strong coupling. Until recently, it was believed that their behavior in the normal state could be described within the framework of the conventional Fermi liquid model.

Gradually accumulating experimental data calls this viewpoint into question. The most evident contradictions with the properties of BCS superconductors and normal metals presented in this article are: (i) linear dependence of the second critical field on temperature, (ii) linear temperature dependence of resistance in the normal state, (iii) linear positive magnetoresistance in strong magnetic field $\omega_c\tau \gg 1$ and (iv) negative magnetoresistance in strong magnetic fields.

Each of these listed effects has, in principle, been previously observed for different classes of

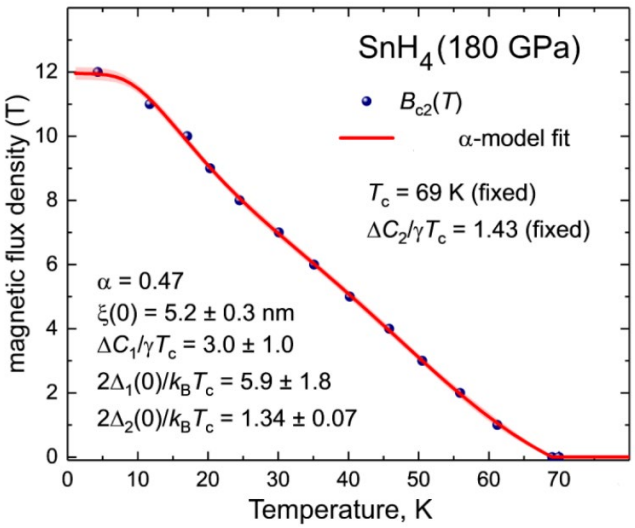

Fig. 7. Example of approximation of the measured dependence $H_{c2}(T)$ within the framework of a two-component so-called alpha-model of SC-condensate. Model parameters are shown in the figure. Adapted from [46], Supplemental information

materials and found its individual explanation. However, collectively these anomalous properties are only found in cuprate HTS [83–85] and still lack a satisfactory microscopic explanation. Such state at $T > T_c$ in cuprates is phenomenologically associated with the so-called "strange metal", and the superconducting state at $T < T_c$ — with a superconductor with moderately strong coupling.

Progress in the synthesis of new superconducting hydrides is occurring so rapidly that it is appropriate to ask whether there is a limit to increasing the critical temperature of superconductivity. In the beginning of the 21st century, V. L. Ginzburg answered this question negatively, referring to the absence of theoretical limitations on reaching a critical temperature of 293 K. Data accumulated to date allows for a more precise assessment. Within the Eliashberg–McMillan theory for dirty superconductors with strong coupling and phonon pairing mechanism, the critical temperature depends on three parameters – the "average" phonon frequency $\langle\omega_{\log}\rangle$, electron-phonon interaction constant λ and Coulomb pseudopotential μ^*.

According to McMillan's semi-empirical formula,

$$k_B T_c \approx \frac{\hbar\omega_{\log}}{1.2}\exp\left[-\frac{1.04(1+\lambda)}{\lambda-\mu^*(1+0.62\lambda)}\right]. \quad (3)$$

This formula, refined by Allen and Dynes for the regime of not too strong coupling $\lambda < 1.5$, with two correction functions $f_1, f_2(\lambda,\omega_{\log},\omega_2,\mu)$, has the following form [86]:

$$k_B T_c \approx f_1 f_2 \frac{\hbar\omega_{\log}}{1.2}\exp\left[-\frac{1.04(1+\lambda)}{\lambda-\mu^*(1+0.62\lambda)}\right], \quad (4)$$

where $\omega_{\log}$ — the logarithmic average frequency and ω_2 — the root mean square frequency.

The Coulomb pseudopotential μ^* in the case of strong coupling decreases approximately by half due to the weakening of the Coulomb interaction by the so-called Tolmachev logarithm [87, 88]:

$$\mu^* = \frac{\mu}{1+\mu\ln(E_F/\hbar\omega_D)}, \quad (5)$$

where μ is the averaged potential of Coulomb interaction between electrons in metal, ω_D — the characteristic phonon energy (for example, Debye frequency). As a result, the Coulomb pseudopotential takes values $\mu^* \approx 0.1$–0.15, determined from numerical calculations.

The electron-phonon coupling constant

$$\lambda = 2\int_0^\infty \frac{\alpha^2 F(\omega)}{\omega} d\omega, \quad (6)$$

logarithmic average frequency

$$\omega_{\log} = \exp\left[\frac{2}{\lambda}\int_0^\infty \frac{\alpha^2 F(\omega)}{\omega}\ln\omega d\omega\right], \quad (7)$$

and root mean square frequency

$$\omega_2 = \sqrt{\frac{1}{\lambda}\int_0^{\omega_{\max}}\left[\frac{2\alpha^2 F(\omega)}{\omega}\right]\omega^2 d\omega} \quad (8)$$

are calculated through the Eliashberg spectral function $\alpha^2 F(\omega)$.

As can be seen from formulas (4), (7), (8), the most important parameter is the electron-phonon coupling constant λ. Hypothetically, in the regime of extremely strong coupling $\lambda \gg 1$, the exponential dependence $T_c(\lambda)$ (4) should transform into a root dependence $T_c \sim \lambda^{1/2}\tilde{\omega}$ [88], where $\tilde{\omega} = \langle\omega^2\rangle^{1/2}$. However, the maximum value λ may be limited by system stability and lattice translational invariance.

The literature has repeatedly discussed possible limitations on the maximum allowable value λ_{max}, related to the violation of the adiabatic

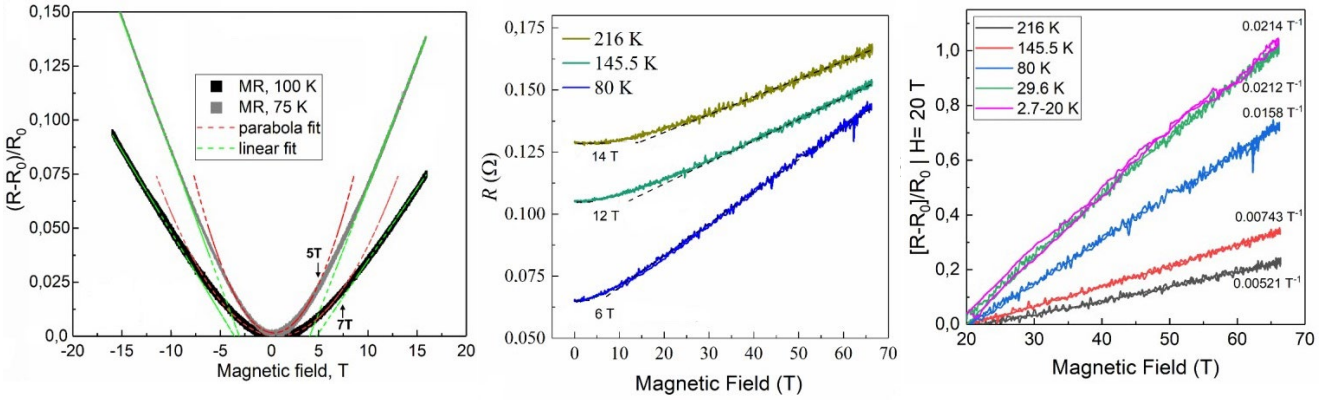

Fig. 8. Normal state resistance dependence for SnH_4 on magnetic field at 180 GPa. $R(H)$ in weak fields up to 16 T at $T = 75$ and 100 K (left panel). $R(H)$ in normal state at $T > T_c = 70$ K (middle panel). Linear part of resistance, normalized to zero field value, plotted in fields above 20 T (right panel). Numbers at curves indicate slope $\Delta R(H) / (R_0 H)$. Due to overheating by eddy currents in pulsed field, the lowest sample temperature reaches ≈ 20 K. Adapted from work [46]

approximation, Migdal's theorem, and Migdal-Eliashberg theory as a whole [89]. Initially, within the framework of the Frohlich Hamiltonian, the limitation $\lambda < 0.5$ was obtained to ensure the stability of the phonon spectrum (positivity of phonon frequency). However, this limitation was obtained for the non-adiabatic case $\hbar\tilde{\omega} \gg E_F$ [89], which is not relevant to most superconductors. Similarly, the bipolaronic instability $\lambda \simeq 1$ [90] corresponds to the non-adiabatic case.

Another limitation, $\lambda = 2$, at first glance, arises from maximizing T_c according to McMillan's formula (3), since the maximum T_c (i.e. $\partial T_c / \partial\lambda = 0$) is achieved precisely at $\lambda = 2$. However, this limitation is also apparent since the formula itself is valid only at $\lambda \leq 1.5$ [88]. To date, significantly larger values of λ, have been determined for many polyhydrides from numerical calculations, for example, 1.84–2.3 (for H_3S, depending on pressure value) [92, 91], 2.06 (for LaH_{10}) [94], 2.41 (for YH_{10}) [94], 2.76 (for LaH_{10}) [93, 95] and, finally, 3.87 (also for $(La, Y)H_{10}$) [96].

Within this same approach, one could address the inverse problem – optimization of the spectral composition of the Eliashberg function. The fact is that in hydrides $\alpha^2F(\omega)$ has two powerful peaks: a peak at low frequencies, $\omega_1 \sim (5-10)$ THz, is associated with acoustic vibrations of metal atoms and almost does not affect the value of T_c, while the high-frequency peak, $\omega_2 \sim 60$ THz, is associated with hydrogen vibration modes [97, 98]. In this context, high pressure promotes increased frequency of hydrogen atom vibrations. The extended intermediate spectral region is almost empty, which negatively affects the values of $\omega_{\log}$ and T_c. The calculated values of the average logarithmic frequency for known polyhydrides are 1080 K (H_3S), 1340 K (YH_{10}), 1210 K (ThH_{10}), 1330 K (YH_6) [54].

As an example of constructing an effective spectral function, let's consider a model rectangular function $\alpha^2F(\omega) = \text{const} = a$ in the frequency interval from $\omega_{(1)}$ to $\omega_{(2)}$ and equal to 0 outside this interval. Then $\omega_{\log} = (\omega_{(1)}\omega_{(2)})^{1/2}$ and $\lambda = 2a\ln(\omega_{(2)} / \omega_{(1)}) = 3.6a \lesssim 3.6$.

According to modern theory, the value of λ_{max} is limited by the violation of lattice translational symmetry and the formation of a gap near the Fermi level [99, 100]. In the latter work, the most "optimistic" numerical estimation of the value $\lambda_{max} \approx 3.0$–$3.7$, was obtained, above which the lattice loses stability. As can be seen, this estimation takes the problem under consideration far beyond the standard BCS theory of weak coupling $\lambda \ll 1$.

From the brief historical review given above, it is evident that in experimentally discovered new superconductors, the coupling constant λ repeatedly exceeded theoretical limits, which turned out to be related to the limited applicability of models. Note that values $\lambda \approx 3$ are already sufficient for achieving superconductivity at room temperature.

Regarding the maximum possible phonon frequency, one can also provide an estimate based on the maximum speed of sound in crystals [101]:

$$\frac{v_s}{c} = \alpha\left(\frac{m_e}{2m_p}\right)^{1/2}, \qquad (9)$$

where α — the fine structure constant, m_e,m_p — the masses of electron and proton, respectively. From this, we obtain $v_s < 36.1 \cdot 10^5$ cm/c and an estimate for the maximum value $\omega_{\log} \sim 2500$ K. Using these estimates for the maximum possible parameters, we get a rough estimate for $T_c^{max} \sim 600$–900 K.

ACKNOWLEDGMENTS

The work of I. T. was partially supported by RSF grant 22-12-00163. D. S. acknowledges financial support for research from the National Natural Science Foundation of China (NSFC, grant No. 1231101238) and Beijing Natural Science Foundation (grant No. IS23017). The measurements were carried out using the equipment of the LPI Shared Facility Center. The research was carried out within the framework of state assignments of NRC Kurchatov Institute and LPI.

REFERENCES

1. E. Wigner and H. B. Huntington, J. Chem. Phys. 3, 764 (1935).
2. N. W. Ashcroft, Phys. Rev. Lett. 21, 1748 (1968).
3. T. W. Barbee et al., Nature 340, 369 (1989).
4. N. W. Ashcroft, Phys. Rev. Lett. 92, 187002 (2004).
5. J. Feng, W. Grochala, T. Jaron, R. Hoffmann, A. Bergara, and N. W. Ashcroft, Phys. Rev. Lett. 96, 017006 (2006).
6. M. I. Eremets, I. A. Trojan, S. A. Medvedev, J. S. Tse, and Y. Yao, Science 319, 1506 (2008). https://doi.org/10.1126/science . 1153282
7. A. P. Drozdov, M. I. Eremets, I. A. Troyan, V. Ksenofontov, and S. I. Shylin, Nature 525, 73 (2015).
8. M. I. Eremets, A. P. Drozdov, Phys. Usp. 186, 1257 (2016).
9. D. V. Semenok, I. A. Troyan, A. G.Ivanova, A. G. Kvashnin, I. A. Kruglov, M. Hanfland, A. V. Sadakov, O. A. Sobolevskiy, K. S. Pervakov, I. S. Lyubutin, K. V. Glazyrin, N. Giordano, D. N. Karimov, A. L. Vasiliev, R. Akashi, V, M. Pudalov, and A. R. Oganov, Materials Today 48, 18 (2021), https://doi.org/10.1016/j.mattod.2021.03.025 .
10. I. A. Troyan, D. V. Semenok, A. G. Ivanova, A. G. Kvashnin, D. Zhou, A. V. Sadakov, O. A. Sobolevskiy, V. M. Pudalov, I. S. Lyubutin, A. R. Oganov, Phys. Usp. 192, 799 (2022).
11. A. P. Drozdov et al., Nature 569, 528 (2019).
12. I. A. Troyan, D. V. Semenok, A. G. Kvashnin, A. V. Sadakov, O. A. Sobolevskiy, V. M. Pudalov, A. G. Ivanova, V. B. Prakapenka, E. Greenberg, A. G. Gavriliuk, I. S. Lyubutin, V. V. Struzhkin, A. Bergara, I. Errea, R. Bianco, M. Calandra, F. Mauri, L. Monacelli, R. Akashi, and A. R. Oganov, Adv. Mater. 33, 2006832 (2021).
13. P. Kong, V. S. Minkov, M. A. Kuzovnikov, A. P. Drozdov, S. P. Besedin, S. Mozaffari, L. Balicas, F. F. Balakirev, V. B. Prakapenka, S. Chariton, D. A. Knyazev, E. Greenberg, and M. I. Eremets, Nat. Commun. 12, 5075 (2021).
14. W. Chen, D. V. Semenok, X. Huang, H. Shu, X. Li, D. Duan, T. Cui, and A. R. Oganov, Phys. Rev. Lett. 127, 117001 (2021).
15. P. W. Anderson, J. Phys. Chem. Solids 11, 26 (1959).
16. A. A. Abrikosov, Fundamentals of the Theory of Metals, Nauka, Moscow (1987).
17. J. Bardeen, L. N. Cooper, and J. R. Schrieffer, Phys. Rev. 108, 1175 (1957).
18. A. A. Abrikosov, L. P. Gorkov, JETP 39, 178 (1960).
19. D. V. Semenok, I. A. Troyan, A. V. Sadakov, D. Zhou, M. Galasso, A. G. Kvashnin, A. G. Ivanova, I. A. Kruglov, A. A. Bykov, K. Y. Terent'ev, A. V. Cherepakhin, O. A. Sobolevskiy, K. S. Pervakov, A. Y. Seregin, T. Helm, T. Förster, A. D. Grockowiak, S. W. Tozer, Y. Nakamoto, K. Shimizu, V. M. Pudalov, I. S. Lyubutin, and A. R.Oganov, Adv. Mater. 34, 2204038 (2022).
20. S. R. W. Legvold, B. J. Green, Beaudry, and J. E. Ostenson, Solid State Commun. 18, 725 (1976).
21. K. Zhang, W. Chen, Y. Zhang et al., Sci. China Phys. Mech. Astron. 67, 238211 (2024), https://doi.org/10.1007/s11433-023-2285-3 .
22. J. Bi, Y. Nakamoto, P. Zhang et al., Nat. Commun. 13, 5952 (2022), https://doi.org/10.1038/s41467-022-33743-6 .
23. W. Chen, X. Huang, D. V. Semenok et al., Nat. Commun. 14, 2660 (2023), https://doi.org/10.1038/s41467-023-38254-6).
24. E. Snider, N. Dasenbrock-Gammon, R. McBride, M. Debessai, H. Vindana, K. Vencatasamy, K. V. Lawler, A. Salamat, and R. P. Dias, Nature 586, 373 (2020).
25. A. F. Goncharov, E. Bykova, M. Bykov, X. Zhang, Y. Wang, S. Chariton, V.B.Prakapenka, and J. S. Smith, J. Appl. Phys. 131, 025902 (2022).
26. A. V. Sadakov, O. A. Sobolevskiy, V. M. Pudalov, UFN 192, 1409 (2022).
27. D. van der Marel and J. E. Hirsch, Int. J. Mod. Phys. 37, 2375001 (2023).
28. N. Dasenbrock-Gammon, E. Snider, R. McBride, H. Pasan, D. Durkee, N. Khalvashi-Sutter, S. Munasinghe, S. E. Dissanayake, K. V. Lawler, A.

Salamat, and R. P. Dias, Nature 615, 244 (2023); https://doi.org/10.1038/s41586-023-05742-0 .

29. Retraction note: https://doi.org/10.1038/s41586-023-06774-2

30. N. S. Pavlov, I. R. Shein, K. S. Pervakov, V.M.Pudalov, and I. A. Nekrasov, JETP Letters 118, 707 (2023).

31. V. Minkov, S. L. Bud'ko, F. F. Balakirev, V. B. Prakapenka, S. Chariton, R. J. Husband, H. P. Liermann, and M. I. Eremets, Nature Commun. 13, 3194 (2022); https://doi.org/10.1038/s41467-022-30782-x .

32. V. Struzhkin, B. Li, C. Ji, X.-J. Chen, V.Prakapenka, E. Greenberg, I. Troyan, A. Gavriliuk, and H.-k. Mao, Matter Radiat. Extremes 5, 028201 (2020).

33. X. Huang et al., Natl. Sci. Rev. 6, 713 (2019).

34. D. Semenok and A. R. Oganov, Nat. Sci. Rev. 6, 856 (2019).

35. V. Struzhkin, Science 351, 1260 (2016).

36. I. A. Troyan, A. Gavroliuk, R. Rüffer, A. Chumakov, A. Mironovich, I. Lyubutin, D, Perekalin, A. P. Drozdov, and M. I. Eremets, Science 351, 1303 (2016).

37. J. E. Hirsch and F. Marsiglio, J. Phys. C 587, 1353896 (2021).

38. Y. Tomioka, M. Naito, and K. Kitazawa, Phys. C: Supercond. 215, 297 (1993).

39. D. M. Gokhfeld et al., J. Appl. Phys. 109, 033904 (2011).

40. D. M. Gokhfeld, Technical Physics Letters 45, 3 (2019).

41. I. S. Lyubutin, in Physical Crystallography, ser. Problems of the Modern Crystallography, Nauka Pub., Moscow (1992), p.326.

42. I. S. Lyubutin and T. V. Dmitrieva, JETP Lett. 21, 59 (1975).

43. R. Bjork and C. R. H. Bahl, Appl. Phys. Lett. 103, 102403 (2013)

44. R. Prozorov et al., Phys. Rev. Appl. 10, 014030 (2018).

45. V. L. Ginzburg, L. D. Landau, JETP 20, 1064 (1950).

46. I. A. Troyan, D. V. Semenok, A. G. Ivanova, A. V. Sadakov, Di Zhou, A. G. Kvashnin, I. A. Kruglov, O. A. Sobolevskiy, M. V. Lyubutina, D. S. Perekalin, T. Helm, S. W. Tozer,

47. M. Bykov, A. F. Goncharov, V. M. Pudalov, and I. S. Lyubutin, Advanced Science 10, 2303622 (2023).

48. N. R. Werthamer, E. Helfand, and P. C. Hohenberg, Phys. Rev. 147, 295 (1966).

49. F. Hunte, J. Jaroszynski, A. Gurevich, D. C. Larbalestier, R. Jin, A. S. Sefat, M. A. McGuire, B. C. Sales, D. K. Christen, and D. Mandrus, Nature 453, 903 (2008); https://doi.org/10.1038/nature07058 .

50. H. Q. Yuan, J. Singleton, F. F. Balakirev, S. A. Baily, G. F. Chen, J. L. Luo, and N. L. Wang, Nature 457, 565 (2009), https://doi.org/10.1038/nature07676 .

51. S. Khim, B. Lee, J. W. Kim, E. S. Choi, G. R. Stewart, and K. H. Kim, Phys. Rev. B 84, 104502 (2011).

52. G. A. Ummarino and A. Bianconi, Cond. Matter 8, 69 (2023); https://doi.org/10.3390/ condmat8030069.

53. C. Wang, S. Yi, and J.-H. Cho, Phys. Rev. B 101, 104506 (2020).

54. K. Kuroki, T. Higashida, and R. Arita, Phys. Rev. B 72, 212509 (2005).

55. D. Semenok, Computational design of new superconducting materials and their targeted experimental synthesis, Doctoral Program in Materials Science and Engineering Thesis, Skoltech, Moscow (2022).

56. H. Jeon, C. Wang, S. Liu, J. M. Bok, Y. Bang, and J.-H. Cho, New J. Phys. 24, 083048 (2022).

57. B. Spivak and F. Zhou, Phys. Rev. Lett. 74, 2800 (1995).

58. V. M. Galitski and A. I. Larkin, Phys. Rev. Lett. 87, 087001 (2001).

59. B. Sacepe, J. Seidemann, F. Gay, K. Davenport, A. Rogachev, M. Ovadia, K. Michaeli, and M.V. Feigel'man, Nature Phys. 15, 48 (2019); https://doi.org/10.1038/s41567-018-0294-6 .

60. A. V. Sadakov, V. A. Vlasenko, D. V. Semenok, Di Zhou, I. A. Troyan, A. S. Usoltsev, and V. M. Pudalov, ArXiv:2311.01318.

61. E. F. Talantsev, Supercond. Sci. and Technol. 35, 095008 (2022); https://doi.org/10.1088/13616668/ac7d78 .

62. D. Sun, V. S. Minkov, S. Mozaffari, Y. Sun, Y. Ma, S. Chariton, V. B. Prakapenka, M. I. Eremets, L. Balicas, and F. F. Balakirev, Nat. Commun. 12, 6863 (2021).

63. D. Semenok, J. Guo, Di Zhou, W. Chen, T. Helm, A. Kvashnin, A. Sadakov, O. Sobolevsky, V. Pudalov, C. Xi, X. Huang, and I. Troyan, ArXiv:2307.11742.

64. F. Bloch, Z. Physik 59, 208 (1930).

65. D. Semenok et al., to be published.

66. C. Castellani, C. DiCastro, H. Fukuyama, P. A. Lee, and M. Ma, Phys. Rev. B 33, 7277 (1986).

67. G. Zala, B. N. Narozhny, and I. L. Aleiner, Phys. Rev. B 64, 214204 (2001).

68. Yanan Zhang, Dajun Su, Yanen Huang, Zhaoyang Shan, Hualei Sun, Mengwu Huo, Kaixin Ye, Jiawen Zhang, Zihan Yang, Yongkang Xu, Yi Su, Rui Li, Michael Smidman, Meng Wang, Lin Jiao, and Huiqiu Yuan, ArXiv:2307.14819v1

69. R. A. Cooper, Y. Wang, B. Vignolle et al., Science 323, 603 (2009).

70. P. Kapitza and E. Rutherford, Proc. R. Soc. London, Ser. A 123, 292 (1929); P.L. Kapitza, Strong Magnetic Fields, Nauka, Moscow (1988).

71. Yu. A. Dreizin, A. M. Dykhne, JETP 63, 242 (1972).

72. C. Heil, S. Di Cataldo, G. B. Bachelet, and L. Boeri, Phys. Rev. 99, 220502(R) (2019).

73. Liu, C. Wang, S. Yi, K. W. Kim, J. Kim, and J.-H. Cho, Phys. Rev. B 99, 140501 (2019).

74. K. Wang and C. Petrovic, Appl. Phys. Lett. 101, 152102 (2012); https://doi.org/10.1063/ 1.4758298.

75. H. Fang, M. Lyu, Hao Su, J. Yuan, Y. Li et al. Preprint https://doi.org/ 10.48550/ arXiv.2301.05918

76. Y. He, J. Gayles, M. Yao, T. Helm, T. Reimann, V. N. Strocov, W. Schnelle, M. Nicklas, Y. Sun, G. H. Fecher, and C. Felser, Nat. Commun. 12, 4576 (2021).

77. J. Richard, P. Monceau, and M. Renard, Phys. Rev. B 35, 4533 (1987).

78. M. Naito1, and S. Tanaka, J. Phys. Soc. Jpn. 51, 228 (1982).

79. A. A. Sinchenko, P. D. Grigoriev, P. Lejay, and P. Monceau, Phys. Rev. B 96, 245129 (2017).

80. A. A. Abrikosov, Phys. Rev. B 58, 2788 (1998).

81. A. A. Abrikosov, Phys. Rev. B 60, 4231 (1999).

82. Jianning Guo, Dmitrii Semenok, Grigoriy Shutov, Di Zhou, Su Chen, Yulong Wang, Kexin Zhang, Xinyue Wu, Sven Luther, Toni Helm, Xiaoli Huang, and Tian Cui, Natl. Sci. Rev. nwae149 (2024); https://doi.org/10.1093/nsr/nwae149 .

83. D. Semenok, J. Guo, Di Zhou, W. Chen, T. Helm, A. Kvashnin, A. Sadakov, O. Sobolevsky, V. Pudalov, C. Xi, X. Huang, and I. Troyan https://arxiv.org/pdf/2307.11742 .

84. A. Legros, S. Benhabib, W. Tabis et al., Nat. Phys. 15, 142 (2019).

85. A. Ataei, A. Gourgout, G. Grissonnanche et al., Nat. Phys. 18, 1420 (2022).

86. R. L. Greene, P. R. Mandal, N. R. Poniatowski et al., Ann. Rev. Cond. Matter Phys. 11, 213 (2020).

87. P. Allen and R. Dynes, Phys. Rev. B 12, 905 (1975); https://doi.org/10.1103/ PhysRevB.12.905.

88. S. Tyablikov, V. Tolmachev, JETP 34, 1254 (1958).

89. V. Z. Kresin, A. G. Ovchinnikov, and S. A. Wolf, Superconducting State, Oxford Univ. Press (2021).

90. M. V. Sadovskii, J. Supercond. Novel Magnetism, 33, 19 (2020).

91. A. S. Alexandrov and A. B. Krebs, Usp. Fiz. Nauk 162, 1 (1992) [Physics Uspekhi 35, 345 (1992)].

92. E. F. Talantsev and K. Stolze, Superconductor Science and Technology 34, 064001 (2021).

93. I. Errea, M. Calandra, C. J. Pickard, J. R. Nelson, R. J. Needs, Y. Li, H. Liu, Y. Zhang, Y. Ma, and F. Mauri, Nature 532, 81 (2016).

94. I. Errea, F. Belli, L. Monacelli et al., Nature 578, 66 (2020); https://doi.org/10.1038/s41586-020-1955-z .

95. F. Peng, Y. Sun, C. J. Pickard, R. J. Needs, Q. Wu, and Y. Ma, Phys. Rev. Lett. 119, 107001 (2017)

96. E. F. Talantsev, Superconductor Science and Technology 33, 094009 (2020).

97. P. Song, Z. Hou, P.Bd . Castro, K. Nakano, K. Hongo, Y. Takano, and R. Maezono, Chem. Mater. 33, 9501 (2021).

98. C. J. Pickard, I. Errea, and M. I. Eremets, Annu. Rev. Cond. Matter Phys. 11, 57 (2020).

99. W. E. Pickett, Rev. Mod. Phys. 95, 021001 (2023), arXiv:2204.05930v4.

100. I. Esterlis, B. Nosarzewski, E. W. Huang, D. Moritz, T. P. Devereux, D. J. Scalapino, and S. A. Kivelson, Phys. Rev. B 97, 140501(R) (2018).

101. E. A. Yuzbashyan and B. L. Altshuler, Phys. Rev. B 106, 054518 (2022).

102. K. Trachenko, B. Monserrat, C. J. Pickard, and V. V. Brazhkin, Sci. Adv. 6, eabc8662 (2020).